

Biofilm Formation by the Fungal Pathogen *Candida albicans*: Development, Architecture, and Drug Resistance

JYOTSNA CHANDRA,¹ DUNCAN M. KUHN,^{1,2} PRANAB K. MUKHERJEE,¹ LOIS L. HOYER,³
THOMAS McCORMICK,⁴ AND MAHMOUD A. GHANNOUM^{1*}

Center for Medical Mycology, University Hospitals of Cleveland, and Department of Dermatology, Case Western Reserve University,¹ Division of Infectious Diseases, University Hospitals of Cleveland,² and Department of Dermatology, Case Western Reserve University,⁴ Cleveland, Ohio 44106, and Department of Veterinary Pathobiology, University of Illinois at Urbana-Champaign, Urbana, Illinois 61802³

Received 14 May 2001/Accepted 27 June 2001

Biofilms are a protected niche for microorganisms, where they are safe from antibiotic treatment and can create a source of persistent infection. Using two clinically relevant *Candida albicans* biofilm models formed on bioprosthetic materials, we demonstrated that biofilm formation proceeds through three distinct developmental phases. These growth phases transform adherent blastospores to well-defined cellular communities encased in a polysaccharide matrix. Fluorescence and confocal scanning laser microscopy revealed that *C. albicans* biofilms have a highly heterogeneous architecture composed of cellular and noncellular elements. In both models, antifungal resistance of biofilm-grown cells increased in conjunction with biofilm formation. The expression of agglutinin-like (ALS) genes, which encode a family of proteins implicated in adhesion to host surfaces, was differentially regulated between planktonic and biofilm-grown cells. The ability of *C. albicans* to form biofilms contrasts sharply with that of *Saccharomyces cerevisiae*, which adhered to bioprosthetic surfaces but failed to form a mature biofilm. The studies described here form the basis for investigations into the molecular mechanisms of *Candida* biofilm biology and antifungal resistance and provide the means to design novel therapies for biofilm-based infections.

Biofilms are studied in a wide range of scientific disciplines including biomedicine, water engineering, and evolutionary biology (3, 10, 14, 15, 22, 23, 33). Biofilms are the most common mode of bacterial growth in nature and are also important in clinical infections, especially due to the high antibiotic resistance associated with them (4, 11, 46). In contrast to the extensive literature describing bacterial biofilms (consult references 34, 35, and 42 for excellent reviews on bacterial biofilms), little attention has been paid to medically relevant fungal biofilms. Transplantation procedures, immunosuppression, the use of chronic indwelling devices, and prolonged intensive care unit stays have increased the prevalence of fungal disease. Fungi most commonly associated with such disease episodes are in the genus *Candida*, most notably *Candida albicans*, which causes both superficial and systemic disease. Even with current antifungal therapy, mortality of patients with invasive candidiasis can be as high as 40% (43). Candidiasis is usually associated with indwelling medical devices (e.g., dental implants, catheters, heart valves, vascular bypass grafts, ocular lenses, artificial joints, and central nervous system shunts), which can act as substrates for biofilm growth. In a multicenter study of 427 consecutive patients with candidemia, the mortality rate for patients with catheter-related candidemia was found to be 41% (31). Forty percent of patients with microbial colonization of intravenous catheters develop occult fungemia, with consequences ranging from focal disease to severe sepsis

and death (2, 31). The tenacity with which *Candida* infects indwelling biomedical devices necessitates their removal to effect a cure. Biofilm formation is also critical in the development of denture stomatitis, a superficial form of candidiasis that affects 65% of edentulous individuals (8, 9). Despite the use of antifungal drugs to treat denture stomatitis, infection is often reestablished soon after treatment (28). These clinical observations emphasize the importance of biofilm formation to both superficial and systemic candidiasis and the inability of current antifungal therapy to cure such diseases.

Our initial work on fungal biofilms involved development and characterization of *C. albicans* biofilms formed on two common bioprosthetic materials: polymethylmethacrylate, which is used in construction of dentures, and silicone elastomer, a model material used for indwelling devices including catheters. The availability of well-characterized, reproducible biofilm models is essential to understanding the nature of *Candida* biofilms and performing studies of biofilm formation and antifungal drug resistance. Recently, using the polymethylmethacrylate biofilm model, we showed that biofilm-grown *C. albicans* cells are highly resistant to antifungal agents such as fluconazole, nystatin, amphotericin B, and chlorhexidine (11), similar to previous observations reported for catheter-associated *C. albicans* biofilms (5, 21). Here, we extend our studies of the model biofilms with emphasis on identifying biofilm growth phases, architectural organization, and correlating antifungal resistance with biofilm development. The use of physiologic parameters and comparison to biofilms from patient specimens demonstrated the clinical relevance of our observations. We also compared *C. albicans* biofilm formation with that of *Saccharomyces cerevisiae* and performed an initial assessment of differential gene expression between planktonic and biofilm-

* Corresponding author. Mailing address: Center for Medical Mycology, University Hospitals of Cleveland and Department of Dermatology, Case Western Reserve University, 11100 Euclid Ave., Cleveland, OH 44106-5028. Phone: (216) 844-8580. Fax: (216) 844-1076. E-mail: mag3@po.cwru.edu.

grown *Candida* cells. Based on our results, we propose that biofilm formation is a highly complex phenomenon, distinct from fungal adhesion. Our data support the conclusion that true biofilms involve both the production of specific extracellular materials and special cellular functions. The information derived from these studies will further our understanding of *Candida* biofilm biology as well as antifungal resistance and may lead to novel therapies for biofilm-based diseases.

MATERIALS AND METHODS

Strains. *C. albicans* strain GDH-2346 was isolated from a denture stomatitis patient (obtained from L. Julia Douglas, University of Glasgow, Glasgow, United Kingdom). *C. albicans* strain M-61 was obtained from an infected intravascular catheter. *S. cerevisiae* strain M-20 was obtained from the stool of a patient on immunosuppressive therapy and admitted to University Hospitals of Cleveland, while strain MRL-138 was a bronchoscopy specimen provided by Lynn Steele More at Christiana Care Health Services, Infectious Disease Laboratory, Wilmington, Del. These fungal strains were grown overnight at 37°C in yeast nitrogen base medium (YNB; Difco Laboratories, Detroit, Mich.) supplemented with 50 mM glucose. The identities of the *C. albicans* and *S. cerevisiae* isolates were determined using the api20C-AUX system, germ tube formation, and urea and nitrate assimilation tests. In these assays, both strains of *S. cerevisiae* were found to be negative for the germ tube and urea and potassium nitrate assimilation tests. Furthermore, these strains were found to be positive for glucose, galactose, maltose, saccharose, and raffinose, but they were negative for 2-keto-D-glucconate, arabinose, xylose, adonitol, xylitol, inositol, sorbitol, N-acetyl-D-glucosamine, cellobiose, and lactose assimilation tests.

Biofilm formation. Biofilms were formed on 1.5-cm² polymethylmethacrylate strips (Dentsply Intl., York, Pa.) as described previously (11). The method for growing biofilms on silicone elastomer disks is described below. A standard inoculum of 1×10^7 cells from overnight cultures of the fungal strains was used to form biofilms in both models. For filamentation experiments, the standard inoculum was added to polymethylmethacrylate strips and then incubated in RPMI 1640 medium (Cellgro; Mediatech). For biofilms grown on silicone elastomer, 1.5-cm-diameter disks of the material (Cardiovascular Instrument Corp., Wakefield, Mass.) were placed in 12-well tissue culture plates and incubated in fetal bovine serum (FBS) for 24 h at 37°C on a rocker. After this pretreatment, disks were washed with phosphate-buffered saline (PBS) to remove residual FBS. To ensure uniform biofilm formation across the strongly hydrophobic disk surface, disks were immersed in 3 ml of standardized cell suspension (1×10^7 cells/ml) and incubated for 90 min at 37°C. Wells were gently washed with PBS to remove nonadherent cells. Subsequently, disks were immersed in YNB medium with 50 mM glucose and incubated for various durations at 37°C on a rocker. Biofilms formed on both polymethylmethacrylate and silicone elastomer materials were quantitated using a tetrazolium XTT [2,3-bis(2-methoxy-4-nitro-5-sulfophenyl)-2H-tetrazolium-5-carboxanilide] reduction assay and dry weight measurement as described previously (11). Disks containing no *Candida* cells served as controls. Assays were carried out in four replicates and were repeated on different days.

Fluorescence microscopy. Polymethylmethacrylate strips or silicone elastomer disks with biofilms were transferred to microscope slides and stained for 1 min with 50 µl of Calcofluor-White (0.05% [vol/vol]; Sigma Chemical Co., St. Louis, Mo.), which fluoresces in the UV range ($\lambda_{\text{max}} = 432$ nm). Stained biofilms were examined under a fluorescence microscope (ZVS-47E microscope; Carl Zeiss, Inc., Oberkochen, Germany).

Confocal scanning laser microscopy (CSLM). At various time points during biofilm formation, polymethylmethacrylate strips or silicone elastomer disks on which biofilms were developing were transferred to a 12-well plate and incubated for 45 min at 37°C in 4 ml of PBS containing the fluorescent stains FUN-1 (10 µM) and concanavalin A-Alexa Fluor 488 conjugate (ConA; 25 µg/ml). FUN-1 (excitation wavelength = 543 nm and emission = 560 nm long-pass filter) is converted to orange-red cylindrical intravacuolar structures by metabolically active cells, while ConA (excitation wavelength = 488 nm and emission = 505 nm long-pass filter) binds to glucose and mannose residues of cell wall polysaccharides with green fluorescence.

After incubation with the dyes, polymethylmethacrylate strips or silicone elastomer disks were flipped and placed on a 35-mm-diameter glass-bottom petri dish (MatTek Corp., Ashland, Mass.). Stained biofilms were observed with a Zeiss LSM510 confocal scanning laser microscope equipped with argon and HeNe lasers and mounted on a Zeiss Axiovert100 M microscope (Carl Zeiss,

Inc.). The objective used was a water immersion C-apochromat lens (40×; numerical aperture of 1.2). Depth measurements were taken at regular intervals across the width of the device. To determine the structure of the biofilms, a series of horizontal (xy) optical sections with a thickness of 0.9 µm, at 0.44-µm intervals, were taken throughout the full length of the biofilm. Confocal images of green (ConA) and red (FUN-1) fluorescence were conceived simultaneously using a multitrack mode. For Calcofluor staining, silicone elastomer disks containing biofilms were gently washed with fresh PBS. Any excess liquid was carefully blotted from the side of the disk, and 50 µl of Calcofluor-White was added to the biofilm surface. Disks were then observed under the confocal microscope as described above.

Antifungal susceptibility. Biofilms were grown on polymethylmethacrylate strips as described previously (11). To measure antifungal susceptibility of *C. albicans* cells grown in developing biofilms, strips were transferred to wells containing different concentrations (ranging from 0.5 to 256 µg/ml) of fluconazole, amphotericin B, nystatin, or chlorhexidine. Strips were incubated for 48 h and metabolic activities of biofilms were measured using the XTT reduction assay as described previously (11). The antifungal susceptibility of planktonic cells was measured using the National Committee for Clinical Laboratory Standards standard M-27A (30) and XTT methods (11) as described previously.

Northern blot analysis. To determine whether expression of *C. albicans* genes is altered as a result of growth as a biofilm on polymethylmethacrylate strips, both *C. albicans* biofilms and planktonic cells were grown in YNB as previously described (11). Biofilm material was scraped from the surface of denture acrylic strips, resuspended in PBS, and centrifuged (3,000 × g) to obtain a pellet containing biofilm matrix. Planktonic cells were similarly collected. Total RNA was extracted from biofilm and planktonic cells according to the procedure described by Collart and Oliviero (13) and analyzed by Northern blot analysis as described previously (26). The blot was probed with a fragment encoding the tandem repeat of *ALS1*, which recognizes multiple genes in the *ALS* family (25). A fragment of the *C. albicans TEF1* gene (41) was used as a control for equal loading as previously described (25).

RESULTS

***C. albicans* biofilm formation proceeds in three distinct developmental phases.** We previously developed a model for denture fungal biofilm growth of *C. albicans* on strips of polymethylmethacrylate (11). In the present study, we investigated temporal development of fungal biofilms using the polymethylmethacrylate biofilm model, as well as one based on silicone elastomer disks. Biofilms grown on polymethylmethacrylate strips were examined by fluorescence microscopy using Calcofluor-White, a UV-excitable dye that binds chitin and beta-glucan and has long been used to highlight fungal cell walls (1). Figure 1 shows that *C. albicans* biofilm formation on polymethylmethacrylate strips progresses in three distinct developmental phases: early (≈ 0 to 11 h), intermediate (≈ 12 to 30 h), and maturation (≈ 38 to 72 h). Initially (0 to 2 h), the majority of *C. albicans* cells were present as blastospores (yeast forms) adhering to the surface of the polymethylmethacrylate strips. At 3 to 4 h, distinct microcolonies appeared on the surface of the strips (Fig. 1a). By 11 h, *C. albicans* communities appeared as thick tracks of fungal growth, due to cell growth and aggregation along areas of surface irregularities. The intermediate developmental phase was characterized by the emergence of predominantly noncellular material (at ≈ 12 to 14 h), which appeared as a haze-like film covering the fungal microcolonies (Fig. 1b). The hazy appearance was due to diffuse staining of the extracellular material with Calcofluor and implied that this material was composed mainly of cell-wall-like polysaccharides. During the maturation phase, the amount of extracellular material increased with incubation time, until *C. albicans* communities were completely encased within this material. At this stage it was difficult to focus on the basal blastospore communities covered by the matrix (Fig. 1c). Fungal commu-

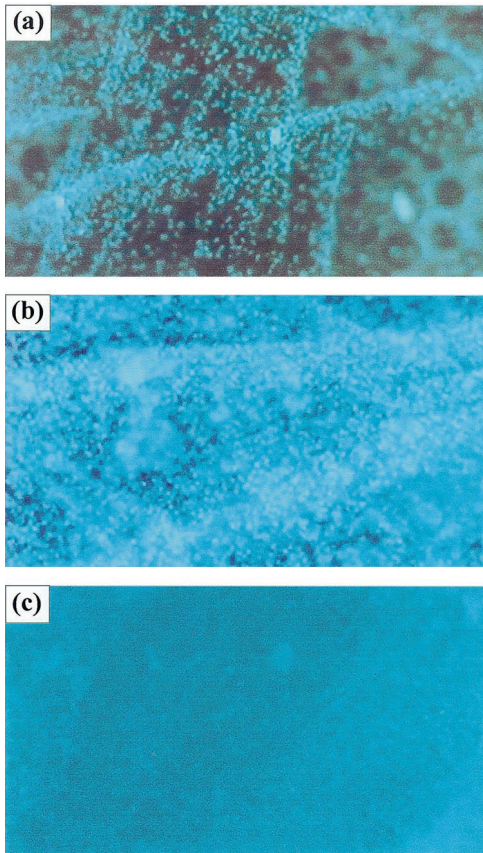


FIG. 1. Development of *C. albicans* biofilm on polymethylmethacrylate strips. Fluorescence microscopy images show the three distinct developmental phases of *C. albicans* biofilms over a 72-h period: early (a), intermediate (b), and maturing (c) phases. Magnification, $\times 10$.

nities and the extracellular material in which they are embedded constitute the biofilm.

These studies were performed on *C. albicans* cells growing in YNB medium, which supports growth of blastospores. *C. albicans* can exist as yeast cells, pseudohyphae, or hyphae. The hyphal forms of *C. albicans* are believed to play an important role in fungal infection (18, 48, 49). Therefore, we repeated our experiments using a different medium, RPMI 1640, which induces hyphal formation in *C. albicans* (26). To initiate biofilm formation, *C. albicans* yeast cells (1×10^7) were added to polymethylmethacrylate strips and incubated in RPMI 1640 medium. After 72 h, biofilms formed in this medium showed no significant difference in terms of dry biomass and metabolic activity, compared to biofilms grown in YNB. In this regard, metabolic activity and dry biomass (optical density at 492 nm [mean \pm standard error of the mean], 0.285 ± 0.009 ; 2.707 ± 0.005 mg/denture piece) of biofilms grown in RPMI 1640 were similar to those grown in YNB (optical density at 492 nm, 0.366 ± 0.054 ; 2.750 ± 0.150 mg/denture piece) ($P > 0.05$ for both comparisons). Unlike the YNB-grown biofilms, which contained mainly yeast forms, the RPMI-grown biofilms consisted mostly of *C. albicans* filaments (data not shown). These data suggested that both yeast and hyphal forms of *C. albicans* were capable of biofilm formation, indicating that biofilm growth was not morphology specific.

We found a similar pattern of biofilm growth on the silicone elastomer substrate model. Fluorescence microscopy showed a much more confluent blastospore layer early in development, followed by the production of extracellular material. The resulting biofilm matrix, although grown in YNB medium, had an abundant component of hyphal elements. However, this silicone elastomer biofilm model incorporates FBS, which is known to promote hyphal formation in *C. albicans* (32). In order to determine if the abundant hyphae observed in silicone elastomer biofilms are induced by FBS, we repeated these experiments by replacing FBS with PBS. Our data showed that biofilms grown in the presence of PBS also contained hyphae, albeit to a lesser extent than that observed in FBS-grown biofilms.

Model biofilms are morphologically similar to those formed in vivo. To determine whether our in vitro model biofilms mimic those formed on bioprosthetic devices in vivo, an infected central venous catheter was obtained from a patient with *C. albicans* fungemia. The catheter was removed and several distal centimeters were cut off and placed in a specimen cup. After the tip had been rolled on a blood agar plate for culture, the distal 1 cm of the catheter was cut off, placed on a glass microscope slide, stained with Calcofluor, and observed under fluorescence microscopy. This examination revealed that the biofilm formed on the infected intravenous catheter was similar in structure to biofilms grown using our silicone elastomer model (data not shown). These data suggest that our in vitro model system is analogous to in vivo events and may be clinically relevant. However, to conclude that the in vitro and in vivo biofilms share the same properties, it will be necessary to study multiple in vivo-derived biofilms and compare the biomass per surface area of the in vitro and in vivo biofilms and to determine the antifungal resistance of the biofilm-grown fungi versus planktonically grown fungi recovered from implants.

It is important to note that similar biofilm morphological patterns were produced in our systems under a variety of environmental parameters (substrates, substrate preconditioning solutions, and growth media). While environmental conditions affect biofilm production, it is possible that certain pathogenic strains of fungi such as *C. albicans* have a special ability to initiate biofilm formation under a wide range of conditions, similar to that seen in some bacteria such as *Pseudomonas fluorescens* (16).

***C. albicans* biofilm has a highly heterogeneous structure.** Biofilm development was further explored using CSLM. We chose this technique instead of scanning electron microscopy because the fixation and dehydration required for scanning electron microscopy severely distort biofilm architecture and shrink any aqueous phase, while CSLM preserves the intact structure of biofilms (36, 44, 45). CSLM examination of *C. albicans* biofilms used a combination of the fluorescent dyes FUN-1 and ConA (both from Molecular Probes, Inc., Eugene, Oreg.). In addition to localizing cells within a specimen, combinations of FUN-1 (a cytoplasmic fluorescent probe for cell viability) and ConA (which selectively binds to mannose and glucose residues present in cell wall polysaccharides) can be used to assess cell viability (20, 29).

Biofilm images were either displayed individually or reconstructed in three-dimensional (3-D) projections. In addition,

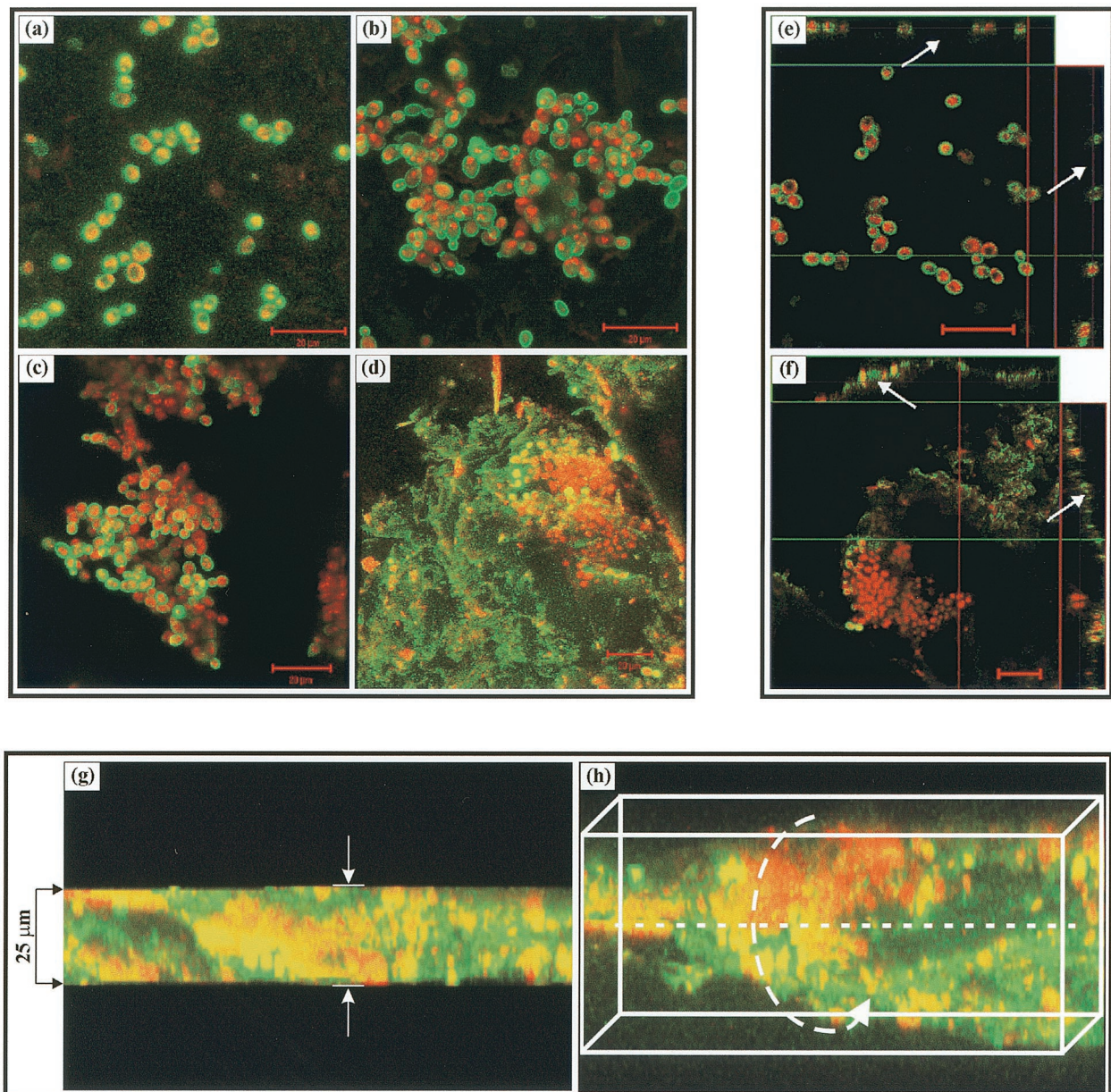


FIG. 2. CSLM images of a *C. albicans* biofilm grown on denture acrylic surface. (a to d) Horizontal (xy) view of reconstructed 3-D images at 0 (a), 8 (b), 11 (c), and 48 (d) h. Bar, 20 μ m. (e and f) Orthogonal images of *C. albicans* biofilms grown to early and maturation phases show that early-phase (0 h) biofilm consisted of mostly yeast cells separated by blank spaces (arrows) (e), while maturation-phase (48 h) biofilm showed metabolically active (red, FUN1-stained) cells embedded in the polysaccharide extracellular material (green, ConA-stained, arrows) (f). (g and h) Thickness of the biofilm ($\approx 25 \mu$ m) can be observed in the side view of the reconstruction (g), while a horizontally tilted image (with false 3-D cubes) shows the heterogeneity of the biofilm (h). Magnification, $\times 40$.

vertical (xz) sections or side views of the 3-D reconstructed images were used to determine biofilm thickness and architecture. Figure 2 shows 3-D reconstruction of images of the early biofilm development phase with individual yeast cells adhering to acrylic strips (Fig. 2a). Intense green fluorescence resulting from ConA binding to polysaccharides outlined the cell walls of the yeast, while the red color due to FUN-1 staining localized in dense aggregates in the cytoplasm of metabolically active cells. Thus, areas of red fluorescence represent metabolically active cells and green fluorescence indicates cell-wall-

like polysaccharides, while yellow areas represent dual staining. By 8 h, *C. albicans* cells increased in density and tended to aggregate (Fig. 2b). Microcolonies of predominantly yeast forms were visible by 11 h (Fig. 2c), while mature biofilms showed fungal cells embedded within the extracellular material (Fig. 2d). These analyses revealed a highly heterogeneous architecture of mature *C. albicans* biofilms in terms of the distribution of fungal cells (indicated by red color) and extracellular material (green coloration). Importantly, no extracellular material could be detected at the early biofilm stage. The lack

of extracellular material was confirmed by orthogonal presentation of the data (Fig. 2e and f). As shown in Fig. 2e, yeast cells in early biofilm development were separated by regions lacking fluorescence, indicating the absence of extracellular material. In contrast, *C. albicans* cells in mature biofilms were encased in extracellular material which appeared as diffuse green fluorescence separate from cell bodies (Fig. 2f). The fact that the biofilm extracellular material stained with ConA, in parallel to the staining pattern of Calcofluor, reinforced the concept that biofilm extracellular material was composed of polysaccharide material. Projection analysis as well as vertical (xz) sectioning (side view) of 3-D reconstructed images also revealed that mature *C. albicans* biofilms have a heterogeneous matrix structure (25 to 30 μm thick), with thin areas of metabolically active cells interwoven with extracellular polysaccharide material (Fig. 2g and h). This appearance is similar to that seen with bacterial biofilm systems (16).

Because silicone elastomer disks have a uniformly flat surface, unlike the irregular surface of polymethylmethacrylate, planar imaging is readily obtainable. *C. albicans* cells grown on silicone elastomer produced a nearly uniform confluent layer of adherent blastospores, which at maturation were several cells thick (approximately 10 to 12 μm ; Fig. 3). Above this layer of cells, profuse matrix (at least \approx 450 μm thick) was apparent which consisted of extracellular material and hyphal elements (Fig. 3a and b). Hyphal elements originating at the base layer pervaded the extracellular material, both in proximity to the blastospores and through the entire thickness (Fig. 3c to f). Graininess of the images is not an artifact, but rather is due to binding of Calcofluor or ConA (depending on the protocol used) to extracellular material, as demonstrated by the projections in Fig. 3. If matrix was physically removed (either by rubbing or vigorous washing of the biofilm surface), a basal layer of blastospores remained and the granularity disappeared (Fig. 3e and f). Based on our studies with the polymethylmethacrylate as well as the silicone elastomer models, a schematic representation of biofilm development on these surfaces is shown in Fig. 4.

***C. albicans* has a greater ability to form biofilms than *S. cerevisiae*.** *S. cerevisiae* is a model microbe for the study of eukaryotic organisms, including fungi like *C. albicans*. Although *S. cerevisiae* has been isolated from clinical conditions (12), its presence is quite rare and the organism is considered relatively nonpathogenic. We sought to determine whether the property of biofilm formation is a characteristic of pathogenic fungi or a general property that can be extended to species such as *S. cerevisiae*. To do this, we compared biofilm formation by *C. albicans* and *S. cerevisiae* using both the polymethylmethacrylate and silicone elastomer models. In the polymethylmethacrylate model, biofilm formed by *S. cerevisiae* had significantly less growth than biofilm formed by *C. albicans*, as determined by dry weight measurements ($P = 0.0008$; Fig. 5a). To rule out the possibility that differences in growth rates may account for the varying ability of these species to form biofilms, we compared their growth profiles, which appeared quite similar (Fig. 5b). The superior ability of *C. albicans* to form biofilms compared to *S. cerevisiae* was confirmed by fluorescence microscopy, which revealed that *C. albicans* formed extracellular material-rich biofilms on polymethylmethacrylate strips (Fig. 5c). In contrast, *S. cerevisiae* adhered to the strips, but its

growth was limited to thin colonies which failed to produce appreciable extracellular material (Fig. 5d). A similar observation was noted for biofilms grown on silicone elastomer disks. Dry weight measurement (3.7 ± 0.001 mg/disk for *C. albicans* and 1.6 ± 0.004 mg/disk for *S. cerevisiae*) as well as fluorescence microscopy analysis of biofilms growing on silicone elastomer disks also showed that while *S. cerevisiae* adhered to the silicone elastomer surface (Fig. 5e), it was unable to form mature biofilms compared to *C. albicans*.

Antifungal resistance increases during biofilm development.

Previous studies have shown that fungal biofilms grown on denture and catheter material become resistant to antifungals (11, 21). A similar resistance pattern was seen with our silicone elastomer model where MICs of fluconazole were 1 and >128 $\mu\text{g}/\text{ml}$ for planktonic and biofilm-grown *C. albicans* cultures, respectively. Since it is plausible that antifungal resistance evolves as the biofilm grows to maturation, we investigated correlations between biofilm development and antifungal susceptibility. MICs of amphotericin B, nystatin, fluconazole, and chlorhexidine were determined for early, intermediate, or mature biofilms. *C. albicans* exhibited low MICs at the early biofilm phase. MICs during this phase were 0.5, 1, 8, and 16 $\mu\text{g}/\text{ml}$ for amphotericin B, fluconazole, nystatin, and chlorhexidine, respectively (Fig. 6). As the biofilms developed, MICs progressively increased (Fig. 6). By 72 h, *C. albicans* cells were highly resistant, with MICs of 8, 128, 32, and 256 $\mu\text{g}/\text{ml}$ for amphotericin B, fluconazole, nystatin, and chlorhexidine, respectively. The progression of drug resistance was associated with the concomitant increase in metabolic activity of developing biofilms (Fig. 6). This indicated that the observed increase in drug resistance was not simply a reflection of lower metabolic activity of cells in maturing biofilms but that drug resistance develops over time, coincident with biofilm maturation. To determine whether *S. cerevisiae* develops antifungal resistance during growth on polymethylmethacrylate strips, MICs of amphotericin B, fluconazole, nystatin, and chlorhexidine were measured at early (0 h) and late (72 h) phases. Our results showed that the susceptibilities of these two phases were similar (Table 1). This was in contrast to *C. albicans* biofilms, for which the MICs increased dramatically between the two time points. Thus, unlike *C. albicans* biofilms, resistance of *S. cerevisiae* to antifungals does not evolve significantly over time when grown on polymethylmethacrylate strips from 0 to 72 h (Table 1).

Differential gene expression under planktonic and biofilm conditions. Since adhesion to bioprosthetic surfaces and cell aggregation are precursors to biofilm formation, it is logical to assume expression of genes involved in these processes changes during the transition from planktonic to biofilm growth. To begin addressing this issue, we investigated the expression profile of *C. albicans* genes belonging to the *ALS* family, which encode proteins implicated in adhesion of *C. albicans* to host surfaces (24). Northern blot analysis of total RNA from planktonic and biofilm-grown *C. albicans* cells showed that there was differential expression of genes between the two growth forms, with additional gene(s) expressed in biofilms (Fig. 7). Further experimentation is required to assess the role of individual *Als* proteins in biofilm formation.

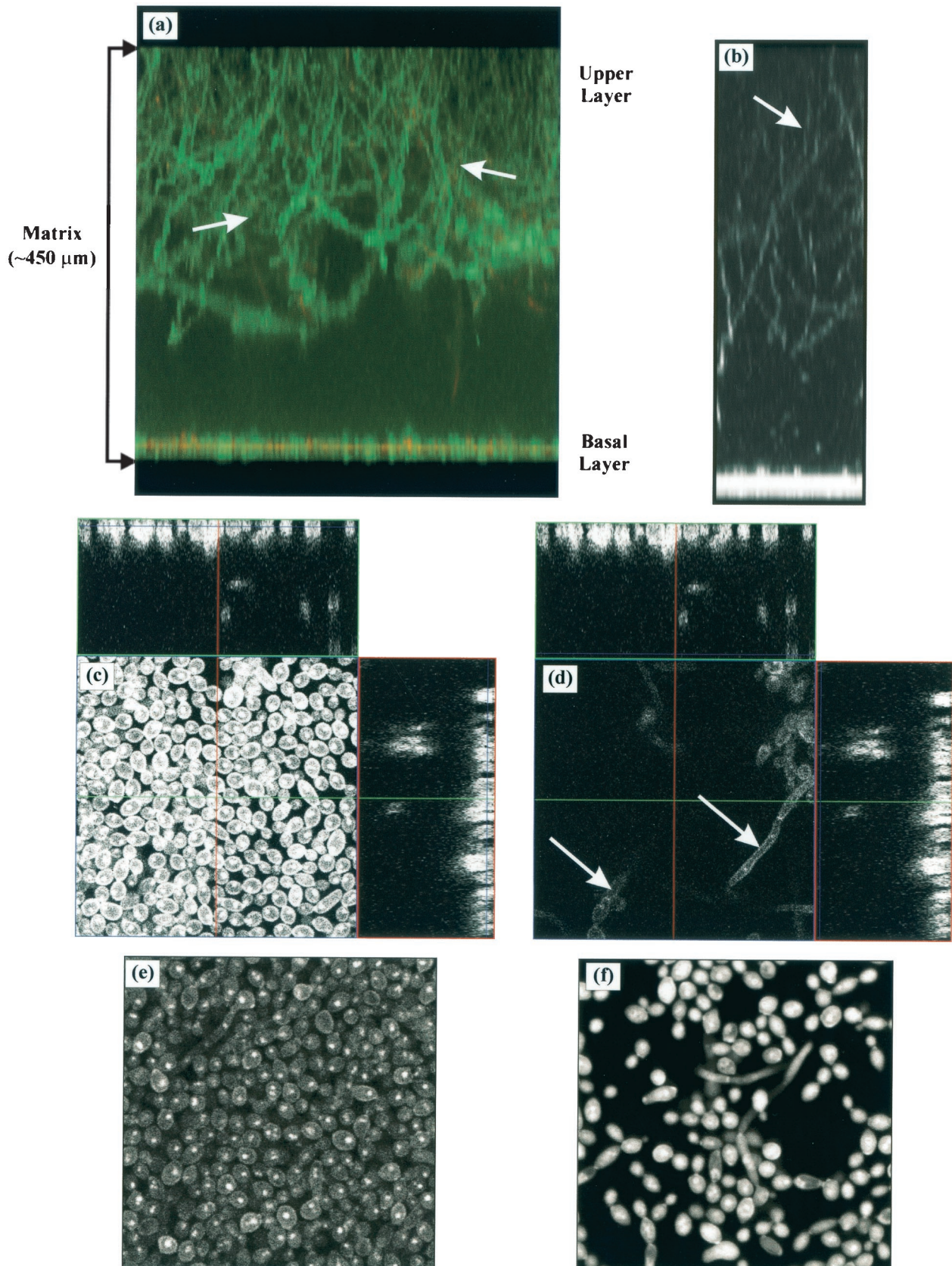


FIG. 3. CSLM images of Calcofluor-stained mature *C. albicans* biofilms formed on silicone elastomer surface. (a and b) Projection (xz or side view) of 3-D reconstructed images showing an approximately 450- μm -thick biofilm with a basal layer (10 to 12 μm thick) consisting of yeast cells and a top layer consisting of hyphal elements (arrow). The extracellular material (ECM) is stained with ConA, resulting in the green color. (c and d) Orthogonal images of the basal (c) and upper layers (d). The ECM-derived haziness seen in mature biofilm (e) is absent when the extracellular material is removed (f). Magnification, $\times 20$.

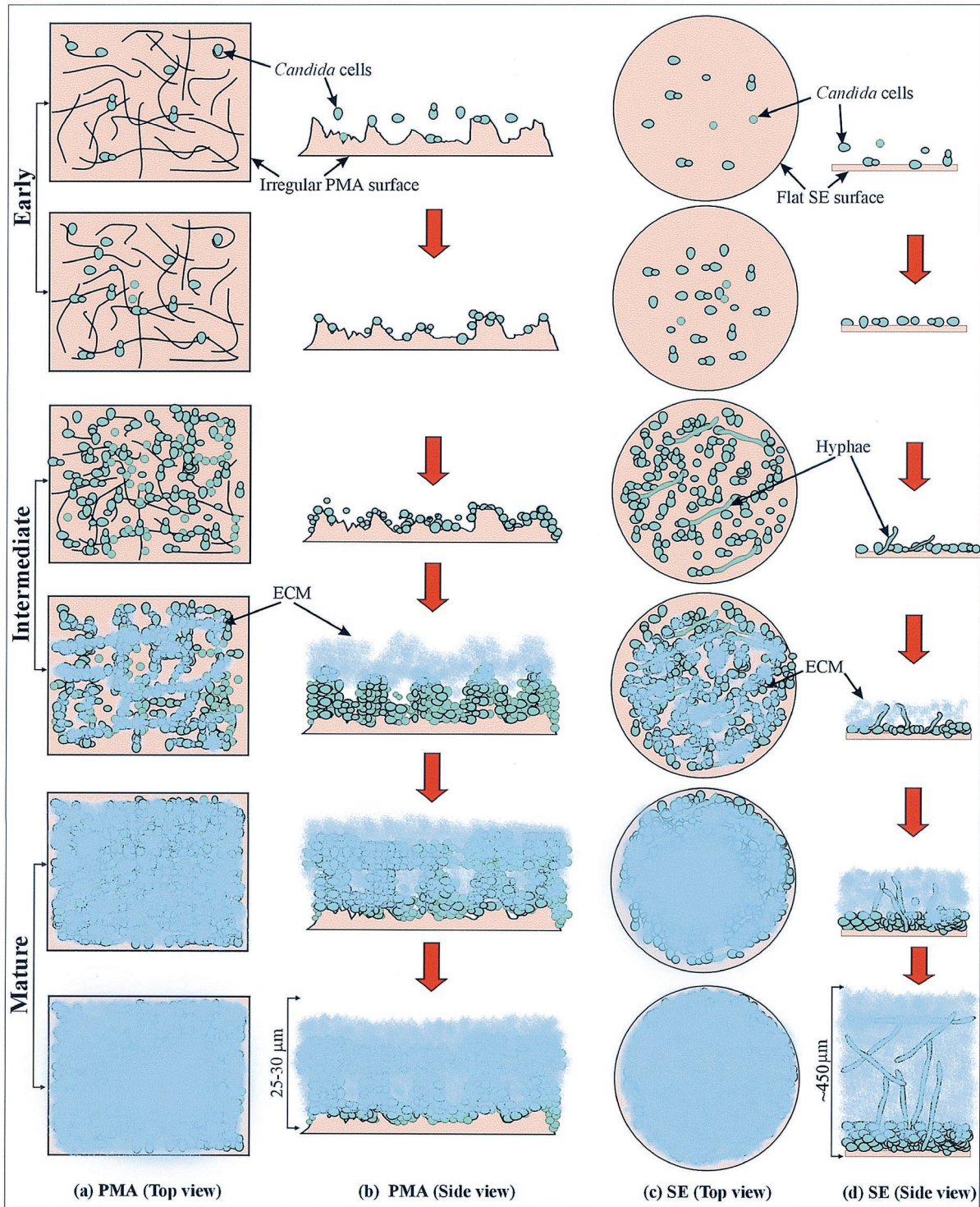


FIG. 4. Schematic representation of biofilm development in *C. albicans*. (a and b) Biofilm grown on polymethylmethacrylate (PMA) strips. (c and d) Biofilm grown on silicone elastomer (SE) disks. Panels a and c represent the substrate seen from the top, while panels b and d show the view from the sides of the PMA strip and SE disk, respectively. ECM, extracellular material.

DISCUSSION

C. albicans biofilm formation proceeds in an organized fashion through the early, intermediate, and maturation phases of development. Similar distinct developmental phases have been

reported for biofilm formation by many bacterial species (16, 34, 42). Thus, microorganisms appear to share common basic steps during biofilm formation. Development of biofilm is closely associated with the generation of matrix, the majority of which is extracellular material. Microscopy strongly suggests

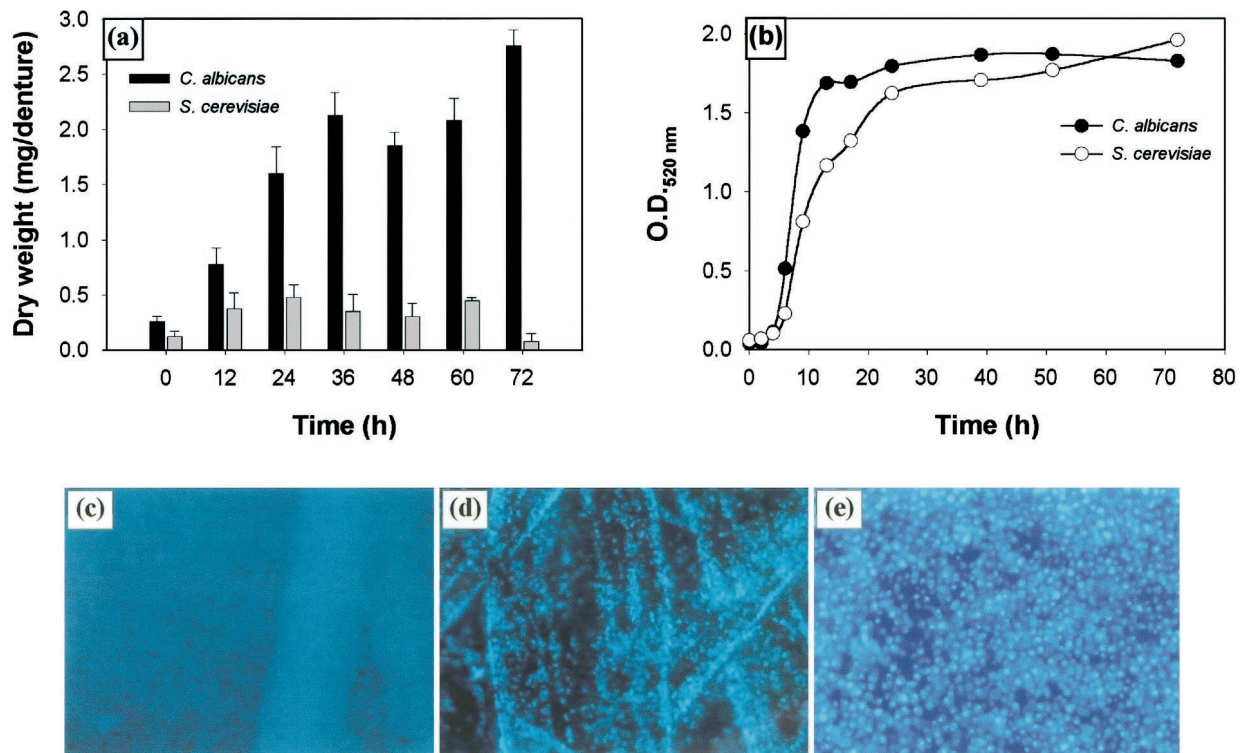


FIG. 5. Comparison of the abilities of *C. albicans* and *S. cerevisiae* to form biofilms. (a) Quantitative measurement of dry weight of biofilms formed by *C. albicans* and *S. cerevisiae*. (b) Growth profiles of planktonic *C. albicans* and *S. cerevisiae*. Fluorescence microscopy images of *C. albicans* (c) and *S. cerevisiae* (d) grown on polymethylmethacrylate strips. (e) Fluorescence micrograph showing *S. cerevisiae* growing on silicone elastomer disk (≈ 3 to $4 \mu\text{m}$ in thickness). Magnification, $\times 10$.

that extracellular material is predominantly composed of cell-wall-like polysaccharides containing mannose and glucose residues, based on staining with dyes that specifically bind these carbohydrates. Mature *C. albicans* biofilms have a highly heterogeneous architecture in terms of distribution of fungal cells and extracellular material. In addition, compared to biofilms grown on the irregular surface of polymethylmethacrylate, those grown on flat hydrophobic surfaces such as silicone elastomer have a distinct biphasic structure composed of an adherent blastospore layer covered by sparser hyphal elements embedded in a deep layer of extracellular material. A similar biphasic distribution was suggested for *C. albicans* biofilms grown on polyvinyl chloride disks (6). Formation of this biphasic architecture could be in response to environmental conditions, such as differences in pH, oxygen availability, and redox potential, prevailing within the biofilm (32, 37, 40, 44, 47). Heterogeneity in the biofilms is another characteristic shared among microorganisms. A “heterogeneous mosaic model” for biofilms has been described, containing stacks of bacterial microcolonies held together by extracellular polymeric substances. Below the stacks is an underlying layer of cells ($\approx 5 \mu\text{m}$ thick) attached to the substratum (44).

Like their bacterial counterparts, biofilm-grown *C. albicans* cells are highly resistant to antimicrobials. Although drug resistance has been shown in *C. albicans* (11, 21) and bacterial biofilms (7, 15), this is the first report correlating the emergence of antifungal resistance with the development of biofilms. Developing *C. albicans* biofilms are associated with an

increasing presence of extracellular material. Extracellular polymeric substance in bacterial biofilms is known to physically interact with antibiotics and is believed to contribute to resistance against these drugs (19, 27). It is unclear if the increase in drug resistance in *C. albicans* biofilms is due to production of extracellular material or due to genetic and biochemical alterations in fungal cells; this is an area for future study. An alternative explanation proposed for antifungal resistance in biofilms is metabolic quiescence of cells. However, this possibility is not likely since biofilm-embedded cells actively metabolize substrates, including XTT and FUN-1.

The biofilm-forming ability of the pathogen *C. albicans* is markedly different from that of *S. cerevisiae*. While the latter is capable of adherence, it fails to progress to a mature biofilm characterized by the presence of extracellular material. A recent report suggested that *S. cerevisiae* forms biofilms in vitro (38). However, the putative *S. cerevisiae* biofilms described in that study do not resemble those formed by *C. albicans* in our standardized model. We believe that these results are in agreement with ours and indicate that, although *S. cerevisiae* adheres to surfaces in a limited way, it fails to form extracellular material-encased biofilms similar to those formed by *C. albicans*. Additionally, our results show that antifungal resistance of adherent *S. cerevisiae* cells did not increase with time. This result was in contrast to *C. albicans* biofilms, where a significant jump in the MICs of drugs was observed between early and mature phase biofilms.

ALS gene expression is differentially regulated during the

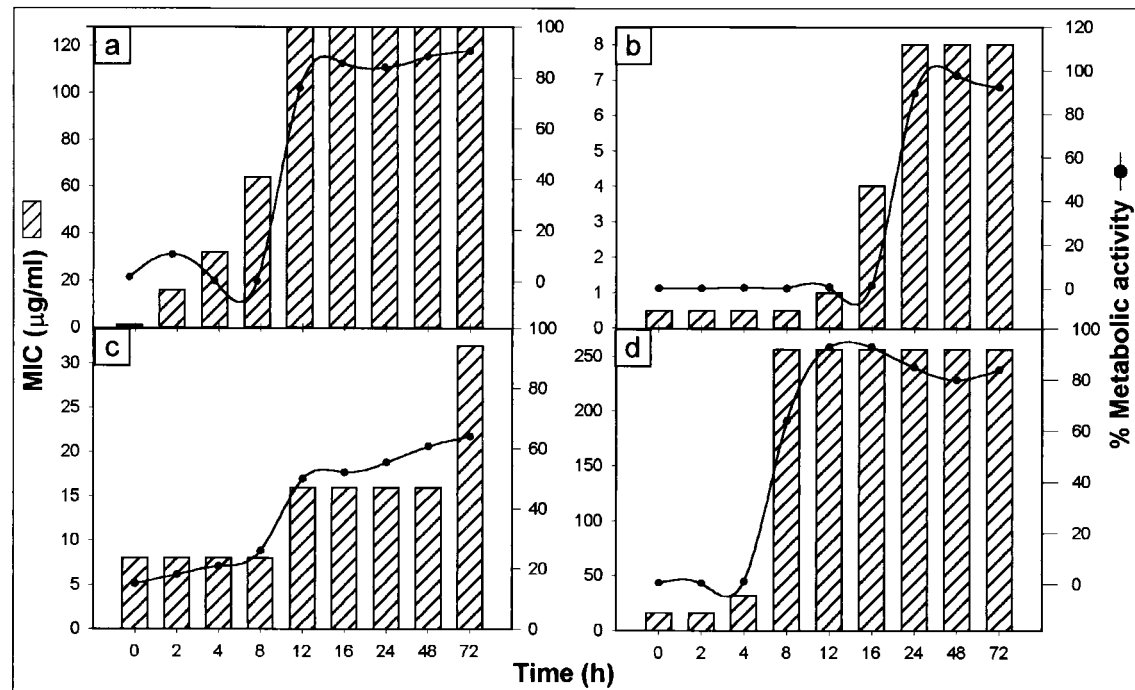


FIG. 6. Correlation of biofilm development and metabolic activity with antifungal resistance. The susceptibilities of *C. albicans* at different stages of biofilm development to fluconazole (a), amphotericin B (b), nystatin (c), and chlorhexidine (d) are represented as histograms. The line curves show percent metabolic activity of growing *C. albicans* biofilms exposed to fluconazole (64 µg/ml), amphotericin B (4 µg/ml), nystatin (8 µg/ml), or chlorhexidine (64 µg/ml). Metabolic activity was normalized to the control without drugs, which was taken as 100%.

transition of *Candida* from a planktonic to biofilm-associated organism. This documentation of differential gene expression between the two growth forms represents a small number of the transcriptional changes that are likely to occur during biofilm formation. The formation of extracellular material associated with *C. albicans* biofilms suggests that genes encoding enzymes involved in carbohydrate synthesis are differentially regulated during biofilm growth. It is also possible that increased expression of drug resistance genes is responsible for the increased MICs observed for *C. albicans* biofilms. Finally, the appearance of a well-defined basal layer of yeast followed by extracellular material production also suggests that genes involved in quorum sensing are important, as is the case with *Pseudomonas* spp. (17, 39). There may also be increased expression of drug resistance genes such as *CDR1*, *CDR2*, and

MDR. Relevant gene regulation can likely only be determined using pathogenic organisms. The well-characterized genome of *C. albicans* and the availability of deletion mutants should allow for rapid evaluation of such possibilities.

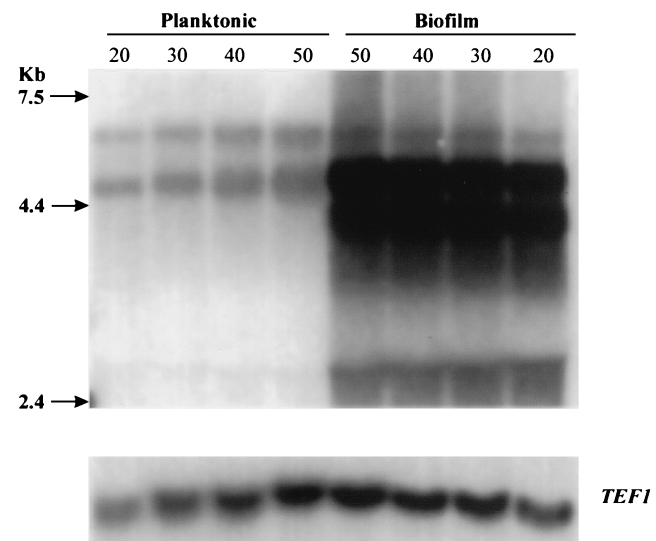


FIG. 7. Northern blot analysis of total RNA extracted from planktonic and biofilm-grown *C. albicans* cells. Total RNA from planktonic and biofilm-grown cells was loaded in various quantities (20, 30, 40, and 50 µg) on a formaldehyde-agarose gel. The resulting Northern blot was probed with a fragment of the *C. albicans* *ALS1* tandem repeats, which hybridized several genes in the family. Probing with a fragment of the *TEF1* gene served as loading control. Molecular size markers (kb) are shown on the left.

TABLE 1. MICs of different agents for *S. cerevisiae* strain MRL-138 and *C. albicans* strain GDH-2346 grown on polymethylmethacrylate strips^a

Antifungal agent	MIC (µg/ml)			
	<i>S. cerevisiae</i>		<i>C. albicans</i>	
	0 h	72 h	0 h	72 h
Amphotericin B	4	4	0.5	8
Chlorhexidine	8	32	16	256
Fluconazole	8	16	1	128
Nystatin	16	32	8	32

^a MICs of different antifungals were determined at 0 h (the time biofilm growth was initiated following adhesion of fungal cells to the substrate, or the early phase) and 72 h (at this time point, the biofilm has matured; the late phase) for both fungi.

Fungal biofilm formation is a complex phenomenon distinct from adhesion. It is best studied using pathogenic species grown on relevant bioprosthetic materials under near-physiologic conditions. Study of such systems will reveal the true nature of fungal biofilms and their biology. Demonstration of common biofilm features (distinct developmental phases, heterogeneous architecture, and drug resistance phenotypes) across different taxa extends the implication of this study beyond fungi to other organized cellular communities. The impact of this information will be widespread, ranging from new environmental microbiology insights to the development of antimicrobials specifically targeted against biofilm-associated infections.

ACKNOWLEDGMENTS

We thank Anna-Liisa Nieminen for helpful discussions and invaluable suggestions.

This work was supported by grants from the U.S. National Institutes of Health (NIH grant nos. AI35097-03 and RO1-DE13992), the Steris Corporation Award for Emerging/Nosocomial Infections (no. 1-88-8225), the Center for AIDS Research at Case Western Reserve University (grant no. AI-36219), an NIH-Infectious Diseases/GeoMed training grant (no. AIO7024; D.M.K.), and a Dermatology Foundation/Janssen Pharmaceutical Research Fellowship (to P.K.M.).

REFERENCES

- Albani, J. R., and Y. D. Plancke. 1999. Interaction between calcofluor white and carbohydrates of alpha 1-acid glycoprotein. *Carbohydr. Res.* **318**:194-200.
- Anaissie, E. J., J. H. Rex, O. Uzun, and S. Vartivarian. 1998. Predictors of adverse outcome in cancer patients with candidemia. *Am. J. Med.* **104**:238-245.
- Austin, J. W., and G. Bergeron. 1995. Development of bacterial biofilms in dairy processing lines. *J. Dairy Res.* **62**:509-519.
- Bagge, N., O. Ciofu, L. T. Skovgaard, and N. Hoiby. 2000. Rapid development *in vitro* and *in vivo* of resistance to ceftazidime in biofilm-growing *Pseudomonas aeruginosa* due to chromosomal β -lactamase. *APMIS* **108**:589-600.
- Baillie, G. S., and L. J. Douglas. 1999. *Candida* biofilms and their susceptibility to antifungal agents. *Methods Enzymol.* **310**:644-656.
- Baillie, G. S., and L. J. Douglas. 1999. Role of dimorphism in the development of *Candida albicans* biofilms. *J. Med. Microbiol.* **48**:671-679.
- Barbeau, J., C. Gauthier, and P. Payment. 1998. Biofilms: infectious agents, and dental unit waterlines: a review. *Can. J. Microbiol.* **44**:1019-1028.
- Budtz-Jorgensen, E. 1990. Etiology, pathogenesis, therapy, and prophylaxis of oral yeast infections. *Acta Odontol. Scand.* **48**:61-69.
- Budtz-Jorgensen, E. 1990. Histopathology, immunology, and serology of oral yeast infections. Diagnosis of oral candidosis. *Acta Odontol. Scand.* **48**:37-43.
- Carr, J. H., R. L. Anderson, and M. S. Favero. 1996. Comparison of chemical dehydration and critical point drying for the stabilization and visualization of aging biofilm present on interior surfaces of PVC distribution pipe. *J. Appl. Bacteriol.* **80**:225-232.
- Chandra, J., P. K. Mukherjee, S. D. Leidich, F. F. Faddoul, L. L. Hoyer, L. J. Douglas, and M. A. Ghannoum. 2001. Antifungal resistance of candidal biofilms formed on denture acrylic *in vitro*. *J. Dent. Res.* **80**:903-908.
- Clemons, K. V., J. H. McCusker, R. W. Davis, and D. A. Stevens. 1994. Comparative pathogenesis of clinical and nonclinical isolates of *Saccharomyces cerevisiae*. *J. Infect. Dis.* **169**:859-867.
- Collart, M. A., and S. Oliviero. 1993. Preparation of yeast RNA, p. 13.12.1-13.12.5. In F. M. Ausubel, R. Bret, R. E. Kingston, D. D. Moore, J. G. Seidman, J. A. Smith, and K. Struhl (ed.), *Current protocols in molecular biology*. John Wiley and Sons, New York, N.Y.
- Costerton, J. W. 2001. Cystic fibrosis pathogenesis and the role of biofilms in persistent infection. *Trends Microbiol.* **9**:50-52.
- Costerton, J. W., P. S. Stewart, and E. P. Greenberg. 1999. Bacterial biofilms: a common cause of persistent infections. *Science* **284**:1318-1322.
- Davey, M. E., and G. A. O'Toole. 2000. Microbial biofilms: from ecology to molecular genetics. *Microbiol. Mol. Biol. Rev.* **64**:847-867.
- Davies, D. G., M. R. Parsek, J. P. Pearson, B. H. Iglesias, J. W. Costerton, and E. P. Greenberg. 1998. The involvement of cell-to-cell signals in the development of a bacterial biofilm. *Science* **280**:295-298.
- Gale, C. A., C. M. Bendel, M. McClellan, M. Hauser, J. M. Becker, J. Berman, and M. K. Hostetter. 1998. Linkage of adhesion, filamentous growth, and virulence in *Candida albicans* to a single gene, *INT1*. *Science* **279**:1355-1358.
- Gilbert, P., J. Das, and I. Foley. 1997. Biofilm susceptibility to antimicrobials. *Adv. Dent. Res.* **11**:160-167.
- Haugland, R. P. 1999. Handbook of fluorescent probes and research chemicals. Molecular Probes, Inc., Eugene, Oreg.
- Hawser, S. P., and L. J. Douglas. 1995. Resistance of *Candida albicans* biofilms to antifungal agents *in vitro*. *Antimicrob. Agents Chemother.* **39**:2128-2131.
- Hellio, C., G. Bremer, A. M. Pons, Y. Le Gal, and N. Bourgougnon. 2000. Inhibition of the development of microorganisms (bacteria and fungi) by extracts of marine algae from Brittany, France. *Appl. Microbiol. Biotechnol.* **54**:543-549.
- Hood, S. K., and E. A. Zottola. 1997. Adherence to stainless steel by food borne microorganisms during growth in model food systems. *Int. J. Food Microbiol.* **37**:145-153.
- Hoyer, L. L. 2001. The *ALS* gene family of *Candida albicans*. *Trends Microbiol.* **9**:176-180.
- Hoyer, L. L., T. L. Payne, and J. E. Hecht. 1998. Identification of *Candida albicans* *ALS2* and *ALS4* and localization of Als proteins to the fungal cell surface. *J. Bacteriol.* **180**:5334-5343.
- Hoyer, L. L., S. Scherer, A. R. Shatzman, and G. P. Livi. 1995. *Candida albicans* *ALS1*: domains related to a *Saccharomyces cerevisiae* sexual agglutinin separated by a repeating motif. *Mol. Microbiol.* **15**:39-54.
- Hoyle, B. D., and J. W. Costerton. 1991. Bacterial resistance to antibiotics: the role of biofilms. *Prog. Drug Res.* **37**:91-105.
- MacEntee, M. I. 1985. The prevalence of edentulism and diseases related to dentures—a literature review. *J. Oral Rehabil.* **12**:195-207.
- Millard, P. J., B. L. Roth, H. P. Thi, S. T. Yue, and R. P. Haugland. 1997. Development of the FUN-1 family of fluorescent probes for vacuole labeling and viability testing of yeasts. *Appl. Environ. Microbiol.* **63**:2897-2905.
- National Committee for Clinical Laboratory Standards. 1997. Reference method for broth dilution antifungal susceptibility testing of yeasts. M-27A. National Committee for Clinical Laboratory Standards, Villanova, Pa.
- Nguyen, M. H., J. E. Peacock, D. C. Tanner, A. J. Morris, M. L. Nguyen, D. R. Snyderman, M. M. Wagener, and V. L. Yu. 1995. Therapeutic approaches in patients with candidemia. Evaluation in a multicenter, prospective, observational study. *Arch. Intern. Med.* **155**:2429-2435.
- Odds, F. C. 1988. *Candida* and candidosis. Bailliere Tindall, London, England.
- Ortega-Morales, O., J. Guezennec, G. Hernandez-Duque, C. C. Gaylarde, and P. M. Gaylarde. 2000. Phototrophic biofilms on ancient Mayan buildings in Yucatan, Mexico. *Curr. Microbiol.* **40**:81-85.
- O'Toole, G., H. B. Kaplan, and R. Kolter. 2000. Biofilm formation as microbial development. *Annu. Rev. Microbiol.* **51**:49-79.
- O'Toole, G. A., L. A. Pratt, P. I. Watnick, D. K. Newman, V. B. Weaver, and R. Kolter. 1999. Genetic approaches to study of biofilms. *Methods Enzymol.* **310**:91-109.
- Palmer, R. J., and C. Sternberg. 1999. Modern microscopy in biofilm research: confocal microscopy and other approaches. *Curr. Opin. Biotechnol.* **10**:263-268.
- Rasmussen, K., and Z. Lewandowski. 1998. Microelectrode measurements of local mass transport rates in heterogeneous biofilms. *Biotechnol. Bioeng.* **59**:302-309.
- Reynolds, T. B., and G. R. Fink. 2001. Bakers' yeast, a model for fungal biofilm formation. *Science* **291**:878-881.
- Singh, P. K., A. L. Schaefer, M. R. Parsek, T. O. Moninger, M. J. Welsh, and E. P. Greenberg. 2000. Quorum-sensing signals indicate that cystic fibrosis lungs are infected with bacterial biofilms. *Nature* **407**:762-764.
- Stoodley, P., D. DeBeer, and H. M. Lappin-Scott. 1997. Influence of electric fields and pH on biofilm structure as related to the bioelectric effect. *Antimicrob. Agents Chemother.* **41**:1876-1879.
- Sundstrom, P., M. Irwin, D. Smith, and P. S. Sypherd. 1991. Both genes for EF-1 alpha in *Candida albicans* are translated. *Mol. Microbiol.* **5**:1703-1706.
- Watnick, P., and R. Kolter. 2000. Biofilm, city of microbes. *J. Bacteriol.* **182**:2675-2679.
- Wey, S. B., M. Mori, M. A. Pfaller, R. F. Woolson, and R. P. Wenzel. 1988. Hospital-acquired candidemia. The attributable mortality and excess length of stay. *Arch. Intern. Med.* **148**:2642-2645.
- Wimpenny, J., W. Manz, and U. Szewzyk. 2000. Heterogeneity in biofilms. *FEMS Microbiol. Rev.* **24**:661-671.
- Wood, S. R., J. Kirkham, P. D. Marsh, R. C. Shore, B. Nattress, and C. Robinson. 2000. Architecture of intact natural human plaque biofilms studied by confocal laser scanning microscopy. *J. Dent. Res.* **79**:21-27.
- Xu, K. D., G. A. McFeters, and P. S. Stewart. 2000. Biofilm resistance to antimicrobial agents. *Microbiology* **146**:547-549.
- Xu, K. D., P. S. Stewart, F. Xia, C. T. Huang, and G. A. McFeters. 1998. Spatial physiological heterogeneity in *Pseudomonas aeruginosa* biofilm is determined by oxygen availability. *Appl. Environ. Microbiol.* **64**:4035-4039.
- Yaar, L., M. Mevarech, and Y. Koltin. 1997. A *Candida albicans* RAS-related gene (*CaRS1*) is involved in budding, cell morphogenesis and hypha development. *Microbiology* **143**:3033-3044.
- Yamada-Okabe, T., T. Mio, N. Ono, Y. Kashima, M. Matsui, M. Arisawa, and H. Yamada-Okabe. 1999. Roles of three histidine kinase genes in hyphal development and virulence of the pathogenic fungus *Candida albicans*. *J. Bacteriol.* **181**:7243-7247.